

# Electromagnetic and thermal analysis of high- $T_c$ superconductor in application of current limiting devices

See Khay Wai · Nasri A. Hamid · Noor Saleha Selamat · Pang Jia Yew · Amir Basha Ismail · Badrol Ahmad

Published online: 1 September 2007  
© Springer Science + Business Media, LLC 2007

**Abstract** Superconducting fault current limiters (SCFCL) offer an attractive way to limit short-circuit currents in power systems. Analysis into electromagnetic and thermal behaviors of superconductor material is crucial in order to develop a novel design concept of a fault current limiter. A new scheme, which can treat electromagnetic field of the type-II superconductor under transient temperature field, is proposed. In this analysis, one of the critical state models, the Bean model was employed to determine the current distribution in the superconductors and effect of magnetic flux flow was also taken into account. Numerical results indicate that the flux flow strongly affects the stability against the quench in Bi-2212 material. High- $T_c$  superconductor material (Bi-2212) was chosen for the current limiting application. In order to investigate characteristics of the current-quenched Bi-2212 bulk, a 2-dimensional heat transfer equation was numerically solved using the finite element simulation. Heat distributions among the superconductor bars were also simulated and by comparing both the experimental and simulated results, it was found that non-uniformities in a current density or a temperature may exist in the quenching of bulk Bi-2212 superconductor.

**Keywords** Superconducting fault current limiter · Type-II superconductor · Bi-2212 superconductor · Finite element simulation

---

S. K. Wai · N. A. Hamid (✉) · N. S. Selamat · P. J. Yew · A. B. Ismail  
College of Graduate Studies, Universiti Tenaga Nasional,  
Kajang 43009 Selangor, Malaysia  
e-mail: Nasri@uniten.edu.my

S. K. Wai · B. Ahmad  
TNB Research Sdn. Bhd., Kawasan Institusi Penyelidikan,  
Jalan Air Hitam,  
Kajang 43000 Selangor, Malaysia

## 1 Introduction

One of promising applications of superconductor in the power system is a fault current limiting device. Since high- $T_c$  superconductor has a large resistance in the normal state compared with ordinary metallic compound superconductors, its quenching due to current can be used as a current limiter by itself. However an operation of a superconductor, especially a thin bulk, under a current-quenching condition gives a large thermal stress to it and may breakdown the bulk due to a local current concentration. From a view point to realize a current limiter which is reliable, self-recovery characteristic and large capacity, it is important to investigate current-quenching characteristics of a thin bulk superconductor.

In this paper, we performed numerical analysis of quench propagation in order to see thermal stability in high  $T_c$  bulk superconductor against thermal disturbance by dealing with electromagnetic field of the type-II superconductor, including the flux flow effect under transient temperature field and their current-resistance characteristics under a current-quenching which was investigated by both experimental and numerical simulation.

## 2 Experimental

In this studies, a highly textured bar-shaped bulk Bi-2212 superconductor elements prepared using a process known as composite reaction texturing (CRT) [1] were used. This technique depends on high aspect ratio magnesium oxide fibers (MgO-f) specifically aligned during the fabrication process. The elements has average critical current of 27 A with transition temperature of around 90 K. The thermal conductivity of the elements at 77 K is  $2 \text{ Wm}^{-1} \text{ K}^{-1}$ , with density closely to 95% of the theoretical density.

Critical current measurements were made in liquid nitrogen (77 K). Current was driven through the superconductor element and the electric field across the superconductor is measured using two electrodes painted onto the surface of the ceramic. The critical current is determined as the current which gives rise to a field of  $1 \mu\text{Vcm}^{-1}$  (the  $1 \mu\text{V}$  criterion).

The experimental setup is shown in Fig. 1. The element was soaked in liquid nitrogen and fed with current using a variable AC source / DC source which operates in both current and voltage source mode. A wave form of current or voltage applied to the element was sine of 50 Hz for one cycle (20 ms). The temporal resistance was calculated from the current ( $I$ ) and voltage ( $V$ ) waveforms using the relation  $R = V/I$ .

The current-resistance characteristic was measured by applying DC current to the element. The variation in applied current ( $I$ ) and the voltage ( $V$ ) that appeared due to quenching were observed. Figure 2 shows the current-resistance characteristic of the element. Resistance of the element first appeared at a current of 27 A and increased exponentially until  $0.7 \Omega$ , and eventually showed saturation characteristic at over 32 A. This temporal behavior of the resistance is due to the flux flow resistivity at above critical current that heated the superconductor element over a critical temperature. The transition from superconducting state to normal state occurs instantly at around the critical temperature, but the dynamic resistance of the element increased gradually with time.

One cycle of 50 Hz sine waveform voltage was applied to the element using the variable AC source to measure the current limiting characteristic. The current was observed to be heavily distorted and limited to about 16 A after 5 ms. A resistance arise and reached its saturated value, and further increased when the current changes its direction.

### 3 Formulation

#### 3.1 Constitutive equation

The macroscopic current distribution in the type-II superconductor is usually described based on the critical state model, where the magnitude of current density is restricted to become  $\pm J_c$  (critical current density) or 0. Constitutive equations to treat the critical state models such as the Bean model have already been proposed [2] as follows;

$$\vec{J} = \sigma_s \vec{E} = \frac{J_c}{|\vec{E}|} \vec{E} \quad |\vec{E}| \neq 0 \quad (1)$$

$$\frac{\partial \vec{J}}{\partial t} = 0 \quad |\vec{E}| = 0 \quad (2)$$

In case under transient temperature field such as quench propagation, however, the effects of temperature change and flux flow on the constitutive equation have to be considered. In order to take the flux flow into account, equation (1) is modified as follows;

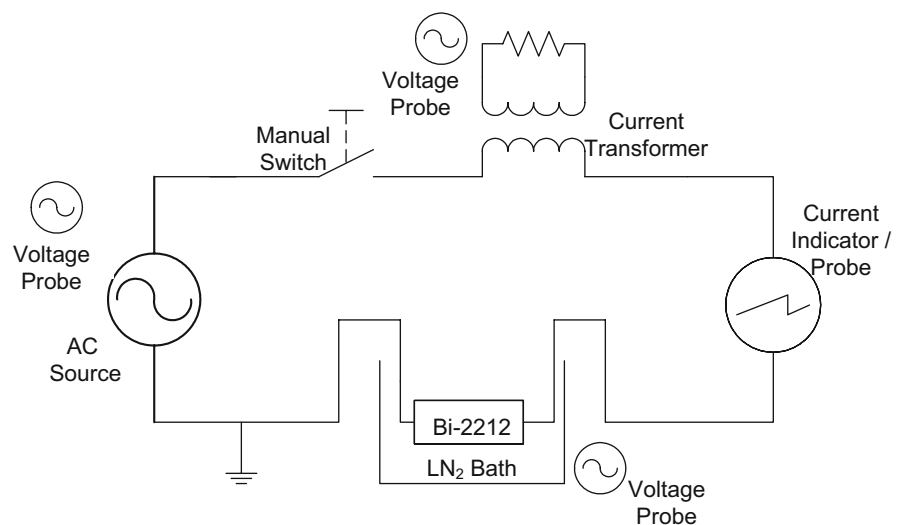
$$\vec{J} = \sigma_s \vec{E} = \frac{J_c}{|\vec{E}|} \vec{E} + \sigma_f \vec{E} \quad |\vec{E}| \neq 0 \quad (3)$$

where  $\sigma_s$  is the equivalent conductivity in the flux flow state, in which;

$$\sigma_f = \sigma_n \frac{B_{c2}}{|\vec{B}|} \quad (4)$$

where  $\sigma_n$  and  $B_{c2}$  are electrical conductivity at normal state and upper critical magnetic field, respectively. Equation (3) means that the flux flow occurs whenever the electrical field exists.

Fig. 1 The experimental setup



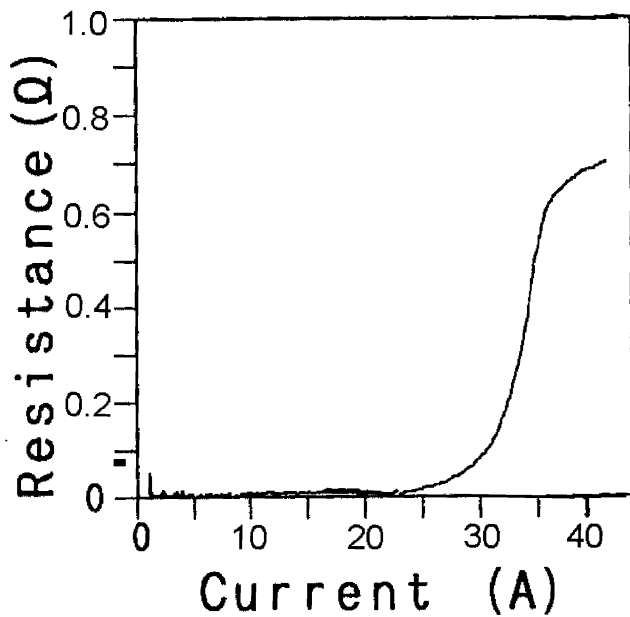


Fig. 2 A current versus resistance characteristic

When the  $J_c$  varies due to the change of temperature, Eqs. (3) and (4) are not available anymore. It is obtained by numerical analysis of fluxoid dynamics that the current density does not change in case of temperature decreasing in spite of the increase of the critical current density. This result means that the magnitude of superconducting current density can vary continuously from  $-J_c$  to  $+J_c$ . When the temperature changes, therefore, the following equations are used.

$$\text{if } |\vec{J}| > J_c \quad \vec{J} = \sigma_s \vec{E} = \frac{J_c}{|\vec{E}|} \vec{E} + \sigma_f \vec{E} \quad (5)$$

$$\text{if } |\vec{J}| \leq J_c \quad \frac{\partial \vec{J}}{\partial t} = 0 \quad (6)$$

When the electrical field becomes 0, the absolute value of current density equals the critical current density as derived from (5). Then Eq. (6) will be satisfied so that the procedure to check the magnitude of electrical field appearing in (1) and (2) could be omitted.

### 3.2 Governing equation for electromagnetic field

In introducing the current vector potential  $T$ , the following equation can be derived based on the Maxwell equations [3, 4], in which;

$$\nabla \times \frac{1}{\sigma} \nabla \times \vec{T} = -\frac{\partial}{\partial t} (\vec{B}_o + \vec{B}_c) \quad (7)$$

where  $B_o$  is the applied field and  $B_c$  is the induced field, and;

$$\vec{B}_c(p) = \mu_o \left( c(p) \vec{T} + \frac{1}{4\pi} \int \vec{n} \cdot \vec{T} \nabla' \frac{1}{R(p,p')} dV(p') \right) \quad (8)$$

where  $C(P)$  is shape function, and  $n$  is normal unit vector.

### 3.3 Governing equation for temperature field

Since the critical current strongly depends on temperature, the temperature distribution in the superconductor has to be evaluated. The equation of heat conduction [5, 6] is expressed by;

$$\rho C_p \frac{\partial \theta}{\partial t} = \nabla \cdot k \nabla \theta + Q_o + Q_j \quad (9)$$

where  $\rho$ ,  $C_p$  and  $k$  are mass density, specific heat and thermal conductivity, respectively.  $Q_o$  is an artificial heat source to induce the quench, while  $Q_j$  is the joule heating source calculated from the electromagnetic analysis.

### 4 Numerical analysis

The temperature dependence of the  $J_c$  and  $B_{c2}$  are usually expressed by the following functions [7, 8];

$$J_c = J_{c0} \left( 1 - \frac{\theta}{\theta_c} \right) \quad (10)$$

$$B_{c2} = B_{c20} \left( 1 - \left( \frac{\theta}{\theta_c} \right)^2 \right) \quad (11)$$

where the subscript 0 indicate 0 K.

In the present analysis, the temperature dependence of normal electrical conductivity and mass density is ignored. Since the Bean model is used, the critical current density does not depend on the magnitude of magnetic field [9].

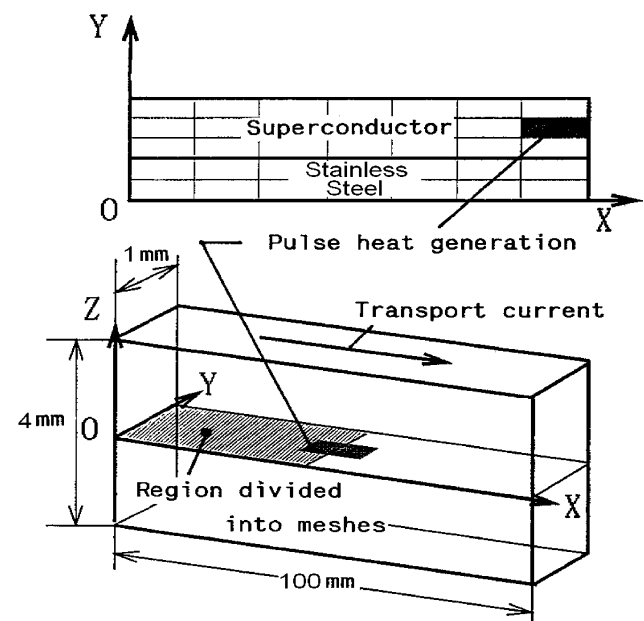
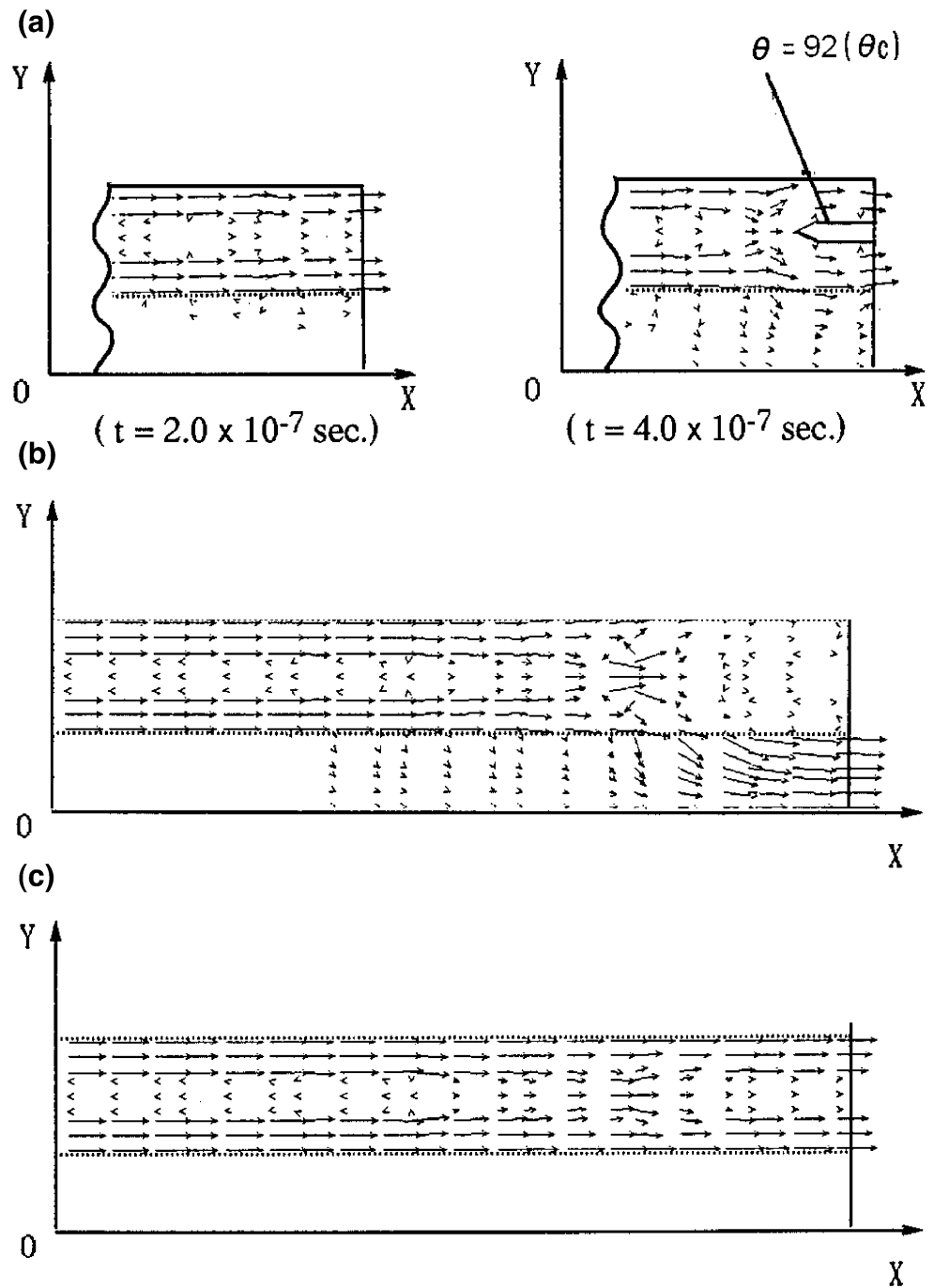


Fig. 3 Finite element meshes of superconductor elements and stainless steel

**Fig. 4** (a) Initiation of current quenching and its development. (b) Current distribution after pulse heating is terminated ( $t=5 \times 10^{-6}$  sec.). (c) Final current distribution after thermal disturbance



Numerical analysis is performed based on the finite element method with eight node isoparametric elements.

As shown in Fig. 3, the current and temperature distributions are two-dimensionally evaluated on the broad face of the cross-section of superconductor elements soaked in liquid nitrogen. Stainless steel bar is mounted beneath the elements with almost the same dimension. A thermal disturbance is produced by giving an artificial pulse heat generation at the center of superconductor element.

In this study, the artificial heat generation of  $10,000 \text{ GW/m}^3 \times 5.4 \mu\text{sec}$  was applied. Figure 4(a)–(c) show the typical dynamic transitions of the current and temperature distributions. Figure 4(a) shows the initiation of current quenching and its development. Transitions of supercurrent and generation of bypass current according to the temperature rise followed by spread of the quenched region are simulated in detail. Figure 4(b),(c) shows the current distribution begins to recover from current quenching be-

cause the joule heating in the stainless steel regions is negligibly small due to large conductivity and as such, the quenched region in the superconductor is cooled effectively. In Fig. 4(b), the supercurrent diffuses from the boundary zones to the center zone of the superconductor in front of the quenched region. The current amplitude is reduced when approaching the quenched region, and mostly flows into the center region of the superconductor while the rest of the current flows into the stainless steel region. This is due to the difference of electrical conductivities between the superconductor and the stainless steel. Moreover, the magnetic field produced by the bypass current reduces the magnitude of the field on the interface of the superconductor element. This change induces the current flowing in the negative x-direction as is predicted by the critical state model. Thus, due to this reversal current, the amplitude of the supercurrent is decreased and, in some case, eddy current is induced in the interface zone [10].

In Fig. 4(c), it is interesting to see some traces of the contracting current even after recovery from current quenching. It indicates that the thermal disturbance induced hysteresis of current distribution in the superconductor. This hysteresis can be explained as follows. Firstly, current distribution is not only distributed in the quenched region but also in the region around the initial temperature. Secondly, due to effective cooling by stainless steel conductors with less joule heating and large diffusivity for heat compared with magnetic flux, temperature distributions both in the superconductor and stainless steel become uniform for a short time. On the contrary the influenced of supercurrent distribution in the region around the initial temperature is unchanged due to small diffusivity of magnetic flux.

## 5 Conclusions

The conclusions from the present study are summarized as follows:

- 1) Spread of current quenching and its recovery after thermal disturbance in type-II superconductor are simulated by the code on the basis of the Bean model.
- 2) The current distribution in the superconductor shows hysteresis against thermal disturbance,
- 3) Electrical conductivity in the flow state strongly affects the quench propagation.

**Acknowledgements** This project has been supported by IRPA Project No. 09-99-03-0024-EA001 from the Ministry of Science, Technology and Innovation, Malaysia and TNB Research Sdn. Bhd.

## References

1. D.R. Watson, M. Chen, J.E. Evetts, *Supercond. Sci. Technol.* **8**, 311 (1995)
2. H. Hashizume, T. Sugiura, K. Miya, S. Toda, *IEEE Trans. Magn.* **28**, 2 (1992)
3. K. Miya, H. Hashizume, *IEEE Trans. Magn.* **24**, 1 (1988)
4. M. Sinder, V. Meerovich, V. Sokolovsky, *IEEE Trans. Appl. Supercond.* **9**, 4 (1999)
5. J.D. Doss, *High-temperature superconductivity* (John Wiley & Sons, United States, 1989)
6. L.C. Thomas, *Heat transfer* (Prentice-Hall, United States, 1992)
7. C.P. Poole Jr., *Superconductivity* (Academic Press, New York, 1995)
8. D. Ruiz-Alonso, T.A. Coombs, A.M. Campbell, *IEEE Trans. Appl. Supercond.* **14**, 4 (2004)
9. J. Bardeen, M.J. Stephen, *Phys. Rev.* **140**, 1197 (1965)
10. B. Zeimetz, K. Tadinada, D.E. Eves, T.A. Coombs, J.E. Evetts, A. M. Campbell, *Supercond. Sci. Technol.* **17**, 657 (2004)